JOURNAL OF SOLID STATE CHEMISTRY 117, 229–235 (1995)

High Pressure Synthesis of Metastable Materials

J. V. Badding, L. J. Parker, and D. C. Nesting

Department of Chemistry, Pennsylvania State University, University Park, Pennsylvania 16802

Received September 4, 1994; accepted November 17, 1994

This paper presents a review of the high pressure synthesis of metastable materials. Many solids synthesized at high pressure can be quenched to ambient conditions, where they may be thermodynamically metastable, yet remain indefinitely kinetically stable. Such routes to metastable solids have attracted much attention, because many of the most technologically important and useful materials are metastable. For geophysics, knowledge of the high pressure–high temperature chemistry of the materials that exist in the interior of the Earth and other planets is crucial to understanding their formation, structure, composition, and evolution. New synthetic opportunities have arisen in this area because of rapid advances in high pressure technology. Using preliminary results from our laboratory, the synthesis of materials at high pressures with modern diamond anvil cells and large volume techniques will be illustrated.

1. INTRODUCTION

High pressure has long been used as a tool to prepare metastable materials (1). For example, despite recent advances in chemical vapor deposition techniques, most of the diamond utilized by industry is still prepared by high pressure synthesis (2). Numerous metastable silicates and oxides have been prepared at high pressure, including chromium dioxide (3), which is used in magnetic recording, and magnesium silicate perovskite (4), which is thought to be the most abundant mineral within the Earth. Silicon can be quenched from high pressure to a dense, metastable metallic form that superconducts at low temperature (5). Quasi-crystalline intermetallic compounds, themselves metastable, can be transformed into metastable, amorphous metals under pressure (6). Recently, metastable nitride glasses have been prepared under pressure (7).

Though high pressure synthesis is an area with a long history, new opportunities have been opened by advances in high pressure technology over the past decade (8). Using diamond anvil cells, it is now possible to compress materials to unprecedented pressures (in excess of 4×10^6 atm or 400 GPa, 1 GPa $\approx$ 10,000 atm) while simultaneously laser-heating them to temperatures as high as 5000 K (9). In contrast, conventional high pressure techniques used in solid state chemistry have typically been limited to pressures on the order of 5 to 10 GPa. It is thus possible for the first time to perform chemical syntheses and physical measurements under conditions as extreme as those that exist in the core of the Earth. Even under less extreme pressure conditions, such large changes can occur in the density, electron configuration, and free energy (as large as in excess of 10^3 kJ/mol) of the elements (Fig. 1) that it can be argued that "new elements" and a "new periodic table" emerge. Extreme changes in chemical equilibria and material properties can result (10), potentially allowing access to a wide range of new compounds, some of which will be quenchable to ambient conditions. New analytical techniques have been developed to probe materials in detail at high pressure, allowing a better understanding of the formation of new compounds (8, 11, 12). Concurrently, there have been advances in larger volume multianvil high pressure techniques that allow the high pressure synthesis of macroscopic amounts of material at pressures up to 35 GPa (13).

We are investigating the high pressure synthesis of carbon based covalent networks and the chemistry of the alkali metals under pressures where they can behave as *d* electron elements (14). Using examples from this research, this paper will illustrate how the diamond anvil cell and the multianvil press can be used to prepare metastable materials and to better understand their formation under pressure. We will describe the synthesis of an amorphous carbon–nitrogen polymer from tetracyanoethylene, a molecule that has not been polymerized by conventional chemical means. We will also discuss the synthesis of new, potentially metastable alloys of the alkali metals.

2. HIGH PRESSURE SYNTHESIS OF METASTABLE COMPOUNDS

The large pressures attainable with modern high pressure techniques allow reaction equilibria to be shifted significantly. The key to whether a compound produced under pressure is quenchable in metastable form to ambi-

0022-4596/95 $12.00

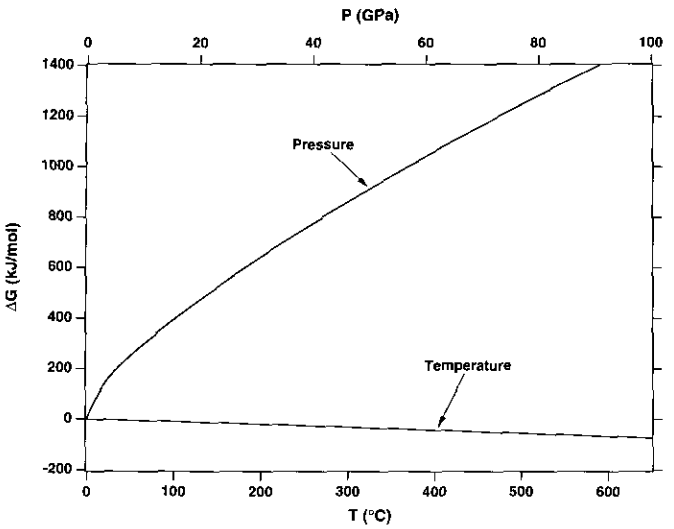

FIG. 1. Gibbs free energy vs temperature (bottom axis) and pressure (top axis) for cesium metal. Much larger changes in free energy are achievable with pressure. The free energy vs pressure curve was derived from an integration of the pressure–volume curve of cesium (51, 52).

ent pressure is the kinetics of the reverse transformation to a stable state. Compounds that require high temperatures for synthesis at high pressure are often quenchable because the kinetics of the reverse transformation are often much slower at room temperature. The archetypal example of this type of reaction is the synthesis of diamond. However, metastable materials can also be prepared by compression at room temperature with no heating. For example, when compressed at room temperature, silicon becomes a metal with the β-tin structure at 11 GPa. When quenched to ambient pressure, this metal transforms to the BC-8 structure (15, 16), which is still tetrahedrally bonded, but denser than semiconducting diamond-structure silicon. As will be discussed, at room temperature high pressure can be used to synthesize polymers that are quenchable to ambient pressure. If a material synthesized at high pressure is not quenchable at room temperature, it can often be quenched at lower temperatures. Examples include the hydrides of elements in the middle of the transition series, which are unstable at room temperature, but can be quenched at liquid nitrogen temperatures (17).

3. HIGH PRESSURE TOOLS

The heart of the diamond anvil cell is a pair of opposed diamond anvils (Fig. 2) that compress a sample contained within a metal gasket (18). Liquids, solids, and gases can be loaded into the diamond cell for reaction at high pressure (8). The diamonds make excellent windows, transparent to x-rays ($\lambda < 0.8$ Å) and from the near UV to the infrared ($\lambda > 200$ nm) (11). X-ray diffraction, a wide range of spectroscopic methods (e.g., Raman, IR, absorbance and reflectance spectroscopies, Brillioun scattering, Mössbauer), and electrical resistivity measurements can be performed in the diamond anvil cell. It is now routine to perform single crystal structure analysis on crystals compressed to high pressure in the diamond cell (19). With synchrotron diffraction techniques (20), it has recently become possible to collect diffraction data at diamond cell pressures on compounds composed of light, weakly scattering elements such as carbon and nitrogen, opening new opportunities for investigating carbon compounds under pressure (21, 22, 23). We have recently developed a diffraction system for the diamond anvil cell that utilizes a curved quartz monochromator to focus X-rays from a rotating anode into a monochromatic, intense beam with low angular divergence, allowing high resolution diffraction patterns to be collected in shorter times than previously possible in the laboratory (24). Compression with a condensed gas surrounding the sample provides a quasi-hydrostatic pressure environment, such that measurements are not degraded by variations in pressure across the sample (8). After removal from the diamond cell, samples can be studied with TEM, SEM, diffraction, microprobe chemical analysis, and many other types of measurements. Thus, the diamond cell is well suited for exploratory synthesis.

Exploratory synthesis in the diamond cell is often followed by the synthesis of larger quantities using a multianvil type press, which can provide quantities of material suitable for NMR, powder diffraction, molecular

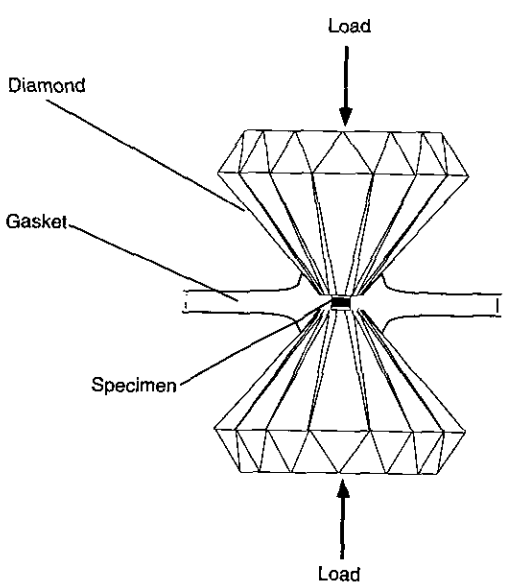

FIG. 2. Diamond anvil cell. Gem quality diamonds with flat culets compress a sample contained within a metal gasket. Sample diameters are generally in the range of 100 to 300 μm.

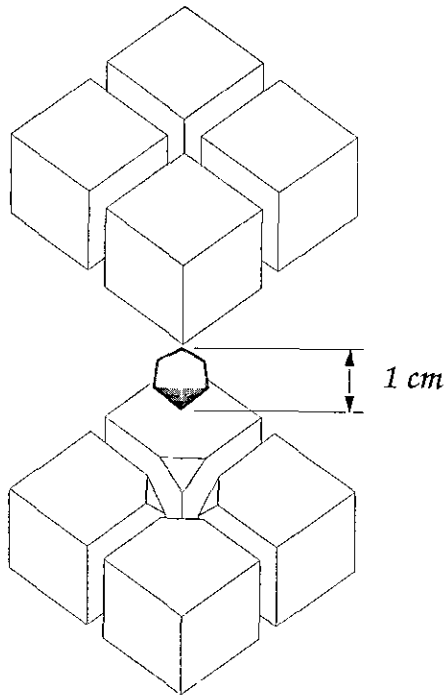

FIG. 3. Octahedral multianvil press. The cubes are truncated along the threefold axis and assembled to compress an octahedron. Load is applied using a large hydraulic press.

weight determination, XPS, and other techniques requiring larger volumes (13). The octahedral multianvil press utilizes a set of eight truncated tungsten carbide cubes to compress a sample embedded in a ceramic octahedron (Fig. 3). Sample size depends on the maximum pressure desired, the maximum load attainable by the press, and the relative amounts of sample and pressure transmitting medium in the octahedron.

4. HIGH PRESSURE SYNTHESIS OF POLYMERS/NETWORKS

New forms of carbon have long stimulated interest. Many different nongraphitic and non-diamond-like carbon networks have been proposed and examined theoretically (25, 26, 27, 28, 29, 30). In view of the very high activation barriers required to break stable C–C bonds, these networks could (like diamond) have kinetic stability and exist in a metastable form. Organic chemists are generating elegant high carbon content molecules with extensive unsaturation that are proposed as precursors for the synthesis of all carbon or very high carbon content networks (31, 32, 33, 59). Recent predictions that there may be superhard phases with extended bonding composed of carbon and nitrogen has led to interest in the synthesis of carbon nitrides (34). A bulk graphitic carbon nitride that incorporates some nitrogen (C_5N) (35, 36, 37) is known. More recently, multiphase carbon nitride films that contain crystalline sp^3 bonded phases have been produced by deposition (38). Amorphous films of composition C_3N_4 have have also been prepared by thermal decomposition of precursors (39).

Since Drickamer's work on high pressure polymerization in the 1960s (40, 41), it has been realized that new types of carbon-based networks might be synthesized under pressure. Molecules containing unsaturation transform under pressure to more saturated networks, which have more extensive intramolecular bonding and, therefore, smaller volume (42). The reactivity of unsaturated molecules under pressure can change because π electron levels can be shifted such that new and potentially more reactive states become available. Because such enormous thermodynamic driving forces can be achieved with current high pressure techniques, virtually any unsaturated system can be polymerized (42). Very stable molecules such as benzene can be polymerized; theoretical predictions suggest that even elemental nitrogen should form a potentially metastable polymer at pressures achievable in the diamond anvil cell (43). This gives a general route to polymerize unsaturated molecules in the solid state and could allow the synthesis of novel polymers and networks that have unprecedented structural features or incorporate functional groups in a novel way.

5. POLYMERIZATION OF TETRACYANOETHYLENE

Tetracyanoethylene (TCNE) belongs to a family of unsaturated molecules containing only carbon and nitrogen. It is well known for its behavior as a Lewis acid in donor–acceptor complexes. TCNE crystallizes in two different structures, a monoclinic form that is stable above 317 K and a cubic form that is stable below 317 K (44). There is no known chemical means of polymerizing TCNE. Plasma polymerization produces an amorphous product (45, 46). Because TCNE contains several unsaturated bonds (four C≡N, one C=C) that could open under pressure, it could serve as a precursor to carbon–nitrogen polymers that would not be restricted to a linear geometry; two- or three-dimensional networks could be envisioned. It has been shown that in the diamond cell TCNE polymerizes irreversibly at room temperature to products that can be recovered to ambient pressure. Infrared spectra have been reported that show that polymerization is likely to involve the nitrile groups (47), but little other information is available about the structure, formation, or properties of the material produced.

To characterize the polymerization process at high pressure we have collected synchrotron diffraction data on compressed TCNE (Fig. 4). Monoclinic TCNE was loaded into a diamond anvil cell with no quasi-hydro-

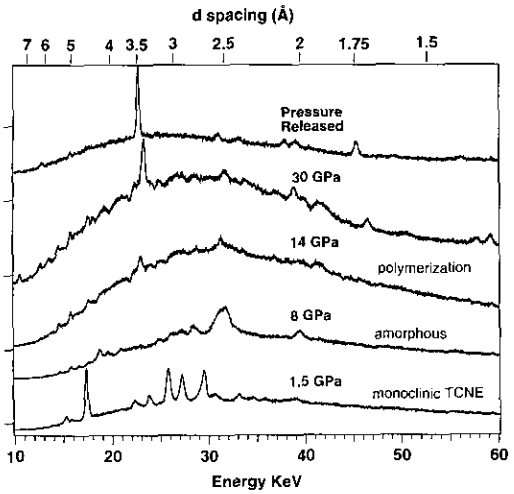

FIG. 4. Diffraction patterns at different pressures for monoclinic TCNE compressed nonhydrostatically in the diamond anvil cell. The patterns were collected at line X17C of the National Synchrotron Light Source using an energy dispersive technique with a 2θ angle of 9°. The top axis shows the d-spacings corresponding to the energies of the bottom axis. By 14 GPa, the diffraction lines due to molecular TCNE disappear. As the diffraction lines from the amorphous phase of molecular TCNE become weak and disappear, lines due to small amounts of ruby used as a pressure calibrant become more prominent. Diffraction from the ruby may have become stronger with increasing pressure because of the breakup of ruby grains into powder. The pattern collected after the pressure was released has only diffraction lines due to ruby

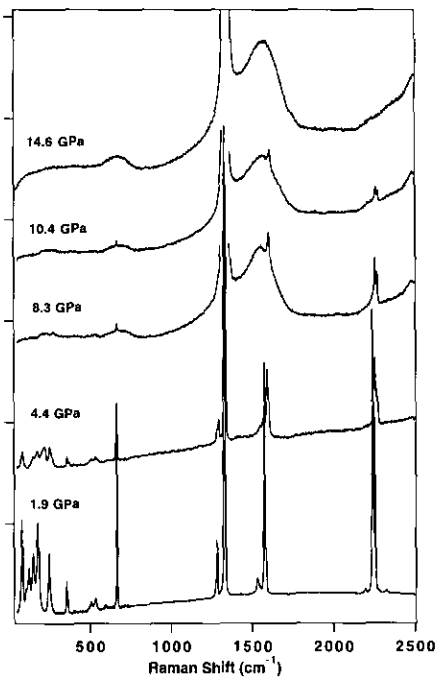

FIG. 5. Raman spectra of TCNE compressed nonhydrostatically in the diamond anvil cell.

static medium. At low pressure (1.5 GPa) TCNE retains the monoclinic structure and is transparent. Earlier work in a relatively low pressure type of large volume apparatus showed that molecular TCNE becomes amorphous at 2.5 GPa (44), which can seen at 8 GPa in the diffraction pattern collected in the diamond cell. By 14 GPa, the sample becomes opaque and the diffraction lines disappear, suggesting that it has become an amorphous or microcrystalline polymer. The recovered sample does not dissolve in solvents, providing further evidence that it has polymerized.

Additional information about the polymerization of TCNE can be obtained from Raman spectroscopy. At 1 GPa, under nonhydrostatic conditions, the Raman spectrum of TCNE (Fig. 5) remains similar to the spectrum at 1 atm (48), but with peak frequencies shifted due to compression. Above 4.4 GPa, the lattice modes of TCNE, located below 300 cm^{-1}, disappear due to amorphization of the sample. Similar behavior was noted in earlier Raman experiments up to a pressure of 6 GPa (48). By 8 GPa most of the sample has reacted, as can be seen from the reduced magnitude of the Raman peaks due to TCNE. The new broad peak at 1580 cm^{-1} is characteristic of structures containing microcrystalline sp^2 carbon. An additional broad peak at 700 cm^{-1} is likely associated with the presence of nitrogen; this feature is never seen in pure carbon films.

Samples compressed to 16 GPa in a multianvil apparatus (13) exhibit an X-ray diffraction pattern that has four broad lines attributable to a microcrystalline graphitic phase. The lines can be indexed according to an expanded hexagonal graphitic structure (a = 2.45 Å, c = 6.90 Å vs. a = 2.456 Å, c = 6.696 Å for graphite). No lines due to the starting material were found. These samples have a black and reflective appearance, suggestive of similarity to disordered carbons. Microprobe analysis shows a chemical composition of C_6N_3, indicating that nitrogen is incorporated. XPS and EELS studies to characterize the bonding in these samples are planned. Like other sp^2 bonded carbon nitrides, this material may serve as a good precursor for the high pressure–high temperature synthesis of potentially superhard sp^3 bonded carbon nitrides.

6. ALLOYS OF NEW ALKALI METALS

Under pressure, the orbital energies of the alkali and alkaline earth metals shift so that they become "new" elements (15). The energy of the n s orbitals of these elements increases more rapidly with pressure than the energy of the more compact, localized $(n - 1)$ d levels. With increasing pressure, the orbital energies cross and the s electrons are transferred to the d levels. The alkali and alkaline earth metals then become d^1 and d^2 metals

with unique electronic structures. The *s–d* transition has been observed for the heavier alkali, alkaline earth, and early transition metals, including Cs, Rb, K, Sr, Ba, Y, and La (14, 49, 50).

Cs provides a dramatic example of this type of transition (51). At ambient pressure Cs is more compressible than condensed Ar (15). At pressures on the order of 3 GPa, its *s* electrons begin to transfer to *d* levels. By 15 GPa, the *s–d* transition is complete and Cs is about four times denser than at ambient pressure, evidence that the extended *s* electrons have been transferred to more localized *d* levels. This high-pressure phase, known as Cs V, has a more complex tetragonal crystal structure than the ambient pressure bcc phase, indicating that directional bonding due to *d* levels is probably important (52). The optical reflectivity and golden color of Cs V demonstrate that *d* electrons are involved in the bonding (53). Due to the increased cohesion associated with more *d*-electron bonding, the melting point of Cs increases with pressure (54). Furthermore, at high pressure Cs superconducts; because superconductivity is never found in simple *s* electron metals, this is further evidence for an electronic structure involving *d* electrons (55). All of these interpretations are supported by theoretical calculations (14, 49, 50, 55). This is a new chemical and physical regime for which the crystal structures, bonding, and properties of the alkali and alkaline earth elements are very different.

Because of the large changes in size and electronic structure of the alkali metals that occur under pressure, there should be significant differences in their chemical reactivity. To demonstrate new chemical behavior for these elements, it would be desirable to find compounds with elements with which they do not react under ambient conditions. For example, with the exception of lithium, there are no known compounds or solid solutions between the alkali metals and the transition elements to the left of gold in the periodic table. There are empirical rules (Miedema's rules) for alloy formation that accurately predict whether a transition metal will alloy with another metal (56). According to these rules, small differences in charge density at the Wigner–Seitz radius and large differences in work function between two metals favor alloy formation. The rules are empirical because the values for the charge density (the cube root of the charge density is actually used) and the work function must be "adjusted" slightly to make the predictions accurate, but the adjusted and true values of these parameters closely follow the same trends. For example, Miedema's rules predict that cesium, rubidium, and potassium form alloys with gold and not with iron because the charge density of gold is less than that of iron (Fig. 6), while its work function is greater. The work functions of the alkali metals and the transition metals differ greatly, which favors alloy formation. However, the differences

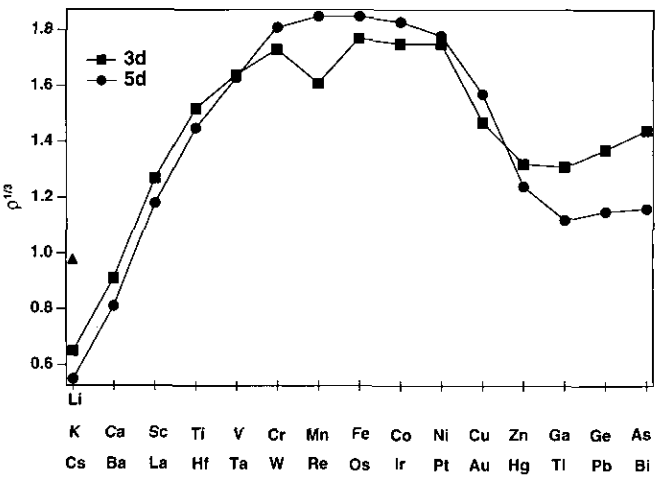

FIG. 6. Cube root of the adjusted charge density at the Wigner–Seitz radius for elements in the third and fifth rows of the periodic table (56).

in charge density are too great to form an alloy. As the alkali metals collapse under pressure and the *s–d* transition occurs, their charge density will increase, which should favor alloy formation with a larger number of transition elements. Gold lies to the right of the peak in the charge density in the transition series (Fig. 6), which occurs for metals in the center of the series (e.g., Fe, Ru, Os). Therefore, the boundary separating the metals that do react with potassium, rubidium, and cesium under pressure (e.g., Au) with those that do not (the rest of the transition series) should move to the left with an increase in pressure. With the diamond cell, the density of the heavier alkali metals can be increased by a factor of approximately 5 at easily achievable pressures, resulting in an increase in the charge density by a factor of 5, such that their charge density should be similar to that of lithium (56). This assumes that the electron remains very delocalized; as it becomes a more localized *d* electron, the charge density might increase even further.

Experiments that demonstrate that the alkali metals behave chemically as new elements are of scientific interest and also should have important geophysical implications. Potassium and rubidium exist within the Earth (57). Current knowledge of the chemistry of these elements at ambient pressure is likely not applicable beyond moderate depths in the Earth, where the pressure is sufficient to induce the *s–d* transition. Specifically, there is considerable current interest in the presence of potassium within the Earth's iron core, which as radioactive ^{40}K could form a source of heat (57). It has been shown that the Earth's core is considerably less dense than would be expected for pure iron under similar pressure and temperature conditions, which implies that a component lighter than iron must be present (57, 58). If potas-

sium can be shown to alloy with iron, it would be a likely candidate for this lighter component.

We have developed techniques which allow the alloy chemistry of metals to be investigated under high pressure. An alkali metal is loaded into the diamond cell together with a transition metal in the form of a thin foil or a powder. This assemblage is then compressed and laser-heated to melt both metals under pressure. X-ray diffraction is used to identify the products. We have performed control experiments that show that, as expected, potassium–gold alloys form in the diamond anvil cell. Figure 7 shows diffraction patterns before and after laser heating of potassium metal and iron foil compressed to 41 GPa in the diamond anvil cell. Diffraction peaks due to both iron and potassium and the rhenium gasket used to contain the sample are present. After laser heating, the iron has developed considerable preferred orientation, indicating that it has melted. No new phase has yet appeared at 40 GPa, but by increasing the pressure or moving to a transition metal with a lower charge density (e.g., Pt, Pd), we expect new alloys to form. These alloys, which are synthesized at high temperature, may be quenchable at room temperature or may require low temperatures to be quenchable.

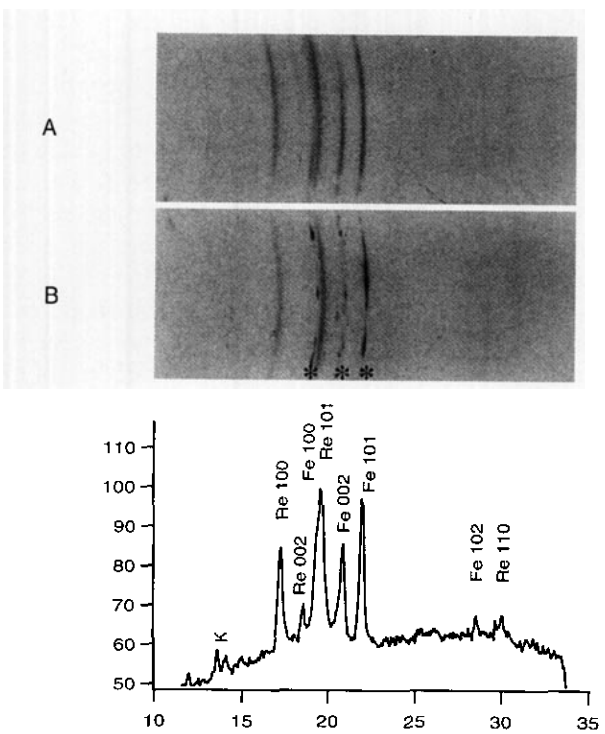

FIG. 7. Diffraction patterns before (A) and after (B) laser heating potassium and iron foil compressed to 41 GPa in the diamond cell. The diffraction patterns were collected on X-ray film in 24 hr using a rotating anode source and a focusing technique (24). The patterns were scanned into a computer and collapsed using the program of Nguyen and Jeanloz (60). Samples were compressed in a rhenium gasket that collapsed down to 75 μm diameter by 41 GPa. Lines due to iron, potassium, and the rhenium gasket were observed. The iron lines (marked with an asterisk) developed preferred orientation, indicating that the iron had melted, but there was no evidence of reaction. The use of a larger gasket hole would reduce the intensity of the rhenium diffraction lines considerably.

7. CONCLUSIONS

Though the number is growing, relatively few chemical studies have been performed with the pressures achievable with the diamond anvil cell and multianvil press, so there is potential for new discoveries. We have shown that under pressure TCNE polymerizes to give an amorphous phase containing substantial amounts of nitrogen. It would be reasonable to expect that many more unsaturated molecules could be polymerized, potentially allowing the synthesis of new classes of carbon-based networks. New, highly unsaturated molecules that are currently under investigation (33), such as tetraethynylmethane, $C(C{\equiv}CH)_4$ (59), could polymerize in interesting ways under pressure. *In-situ* high pressure characterization techniques will be important in understanding the effect of reaction conditions on the polymerization process.

The size and electronic structure of the alkali and alkaline earth metals are sufficiently different under pressure that many new compounds should form. We have discussed the formation of new metallic alloys of the alkali and alkaline earth metals with the transition elements, but the nonmetal chemistry should also be different, at least in bonding situations where the *d* orbitals of the alkali metal are populated. Investigation of this chemistry is possible with current high pressure technology.

ACKNOWLEDGMENTS

We thank Y. Fei of the Geophysical Laboratory, Carnegie Insititution of Washington, and the Center for High Pressure Research for assistance with the multianvil experiments. The synchrotron diffraction patterns were collected at line X17C of the National Synchrotron Light Source. This research was supported by the David and Lucile Packard Foundation, the National Science Foundation, and the Petroleum Research Fund.

REFERENCES

1. J. B. Goodenough, J. A. Kafalas, and J. M. Longo, *in* "Preparative Methods in Solid State Chemistry" (P. Hagenmüller, Ed.), p. 1. Academic Press, New York, 1972.
2. "Report of the Committee on Superhard Materials, Status and Applications of Diamond and Diamond-Like Materials: An Emerging Technology." National Academy Press, Washington DC, 1990.
3. G. Demazeau, *Chem. Scr.* **28,** 21 (1988).
4. L. Liu and W. A. Bassett, "Elements, Oxides, and Silicates." Oxford Univ. Press, New York, 1986.
5. T. V. Valyanskaya and G. N. Stepanov, *in* "High Pressure Science and Technology—1993" (S. C. Schmidt, J. W. Shaner, G. A. Samara, and M. Ross, Eds.), p. 687. Am. Inst. of Phys., New York, 1994.

6. R. R. Winters and W. S. Hammack, *Science* **260,** 202 (1993).
7. T. Grande, J. R. Holloway, P. F. McMillan and C. A. Angell, *Nature* **369,** 43 (1994).
8. H. K. Mao, *in* "Simple Molecular Systems at Very High Density" (A. Polian, P. Loubeyre, and N. Boccara, Eds.), p. 221. Plenum, New York, 1989.
9. R. J. Hemley, P. M. Bell, and H. K. Mao, *Science* **237,** 605 (1987).
10. R. Jeanloz, *Ann. Rev. Phys. Chem.* **40,** 237 (1989).
11. A. Jayaraman, *Rev. Mod. Phys.* **55,** 65 (1983).
12. A. Jayaraman, *Rev. Sci. Instrum.* **57(6),** 1013 (1986).
13. E. Ohtani, T. Irifune, W. O. Hibberson, and A. E. Ringwood, *High Temp.–High Press.* **19,** 523 (1987).
14. A. K. McMahan, *Physica* **139/140B,** 31 (1986).
15. D. A. Young, "Phase Diagrams of the Elements." Univ. of Calif. Press, Berkeley, CA, 1991.
16. J. Z. Hu and I. L. Spain, *Solid State Comm.* **51,** 263 (1984).
17. J. V. Badding, R. J. Hemley, and H. K. Mao, *Science* **253,** 421 (1991).
18. A. P. Jephcoat, H. K. Mao, and P. M. Bell, *in* "Hydrothermal Experimental Techniques" (G. C. Ulmer and H. L. Barnes, Eds.), p. 469, Wiley, New York, 1987.
19. R. M. Hazen and L. W. Finger, "Comparative Crystal Chemistry." Wiley, New York, 1982.
20. C. T. Prewitt, P. Coppens, J. C. Philips, and L. W. Finger, *Science* **238,** 312 (1987).
21. J. V. Badding, H. K. Mao, and R. J. Hemley, *EOS Trans. Am. Geophys. Union.* **71,** 1620 (1990).
22. J. V. Badding, H. K. Mao, and R. J. Hemley, *Solid State Commun.* **77,** 801 (1990).
23. H. K. Mao, Y. Wu, R. J. Hemley, L. C. Chen, J. F. Shu, and L. W. Finger, *Science* **246,** 649 (1989).
24. T. Atou and J. V. Badding, *Rev. Sci. Inst.*, in press.
25. M. A. Tamor and K. C. Hass, *J. Mater. Res.* **5,** 2273 (1990).
26. M. Kertesz and R. Hoffmann, *J. Solid State Chem.* **54,** 313 (1984).
27. R. L. Johnston and R. Hoffmann, *J. Am. Chem. Soc.* **111,** 810 (1989).
28. K. M. Merz, R. Hoffmann, and A. Balaban, *J. Am. Chem. Soc.* **109,** 6742 (1987).
29. M. O'Keefe, G. Adams, B. Sankey, and O. F. Sankey, *Phys. Rev. Lett.* **68,** 2325 (1992).
30. A. Y. Liu, M. L. Cohen, K. C. Hass, and M. A. Tamor, *Phys. Rev. B Condens. Matter* **43,** 6742 (1991).
31. A. H. Alberts and H. Wynberg, *J. Chem. Soc. Chem. Commun.*, 748 (1988).
32. T. X. Neenan and G. M. Whitesides, *J. Org. Chem.* **53,** 2489 (1988).
33. F. Diederich and Y. Rubin, *Angew. Chem. Int. Ed. Engl.* **31,** 1101 (1992).
34. A. Y. Liu and M. L. Cohen, *Phys. Rev. B* **41,** 10,727 (1990).
35. T. Sekine, H. Kanda, Y. Bando, M. Yokoyama, and K. Hojou, *J. Mater. Sci. Lett.*, 1376 (1990).
36. R. B. Kaner, J. Kouvetakis, C. E. Warble, M. L. Sattler, and N. Bartlett, *Mater. Res. Bull.* **22,** 399 (1987).
37. J. Kouvetakis, R. B. Kaner, M. L. Sattler, and N. Bartlett, *J. Chem. Soc. Chem. Commun.*, 1758 (1986).
38. C. Niu, Y. Z. Lu, and C. M. Lieber, *Science* **261,** 334 (1993).
39. J. Kouvetakis, A. Bandari, M. Todd, and B. Wilkens, *Chem. Mater.*, 811 (1994).
40. H. G. Drickamer and C. W. Frank, "Electronic Transitions and the High Pressure Chemistry and Physics of Solids." Chapman & Hall, London, 1973.
41. V. C. Bastron and H. G. Drickamer, *J. Solid State Chem.* **3,** 550 (1971).
42. M. Nicol and G. Z. Yin, *J. Phys. Colloq.* **C8,** 163 (1984).
43. C. Mailhiot, L. H. Yang, and A. K. McMahan, *Bull. Am. Phys. Soc.* **38,** 1496 (1993).
44. W. L. Chaplot and R. Mukhopadhyay, *Phys. Rev. B* **33,** 5099 (1986).
45. Y. Osada, Q. S. Yu, H. Yasunaga, F. S. Wang, and J. Chen, *J. Appl. Phys.* **64,** 1476 (1988).
46. Y. Osada, Q. S. Yu, H. Yasunaga, and Y. Kagami, *J. Polym. Sci. Polym. Chem.* **27,** 3799 (1989).
47. H. Yamawaki, K. Aoki, Y. Kakudate, M. Yoshida, S. Usuba, and S. Fujiwara, *Chem. Phys. Lett.* **198,** 183 (1992).
48. S. L. Chaplot, A. Mierzejewski, and G. S. Pawley, *Mol. Phys.* **56,** 115 (1985).
49. A. K. McMahan, *Phys Rev. B* **29,** 5982 (1984).
50. M. Ross and A. K. McMahan, *Phys. Rev. B* **26,** 4088 (1982).
51. K. Takemura, O. Shimomura, and H. Fujihisa, *Phys. Rev. Lett.* **15,** 2014 (1991).
52. K. Takemura and K. Syassen, *Phys. Rev. B* **32,** 2213 (1985).
53. K. Syassen, *Phys. Rev. Lett.* **49,** 1776 (1982).
54. R. Boehler and C. S. Zha, *Physica* **139/140B,** 233 (1986).
55. J. Wittig, *Mater. Res. Soc. Symp. Proc.* **22,** 17 (1984).
56. A. K. Niessen, F. R. de Boer, R. Boom, P. F. de Chatel, W. C. M. Mattens, and A. R. Miedema, *CALPHAD: Comput. Coupling Phase Diagrams Thermochem.* **7,** 51 (1983).
57. L. Liu, *Geophys. Res. Lett.* **13,** 1145 (1986).
58. R. Jeanloz, *Ann. Rev. Earth Planet. Sci.* **18,** 375 (1990).
59. K. S. Feldman and C. M. Kraebel, *J. Am. Chem. Soc.* **115,** 3846 (1993).
60. J. Nguyen and R. Jeanloz, *Rev. Sci. Instrum.* **64,** 3456 (1993).